Journal of Alloys and Compounds 489 (2010) 429–436

Contents lists available at ScienceDirect

Journal of Alloys and Compounds

journal homepage: www.elsevier.com/locate/jallcom

Review

Study of relaxations in epoxy polymer by thermally stimulated depolarization current (TSDC) and dielectric relaxation spectroscopy (DRS)

Hichem Smaoui[a,b,*], Mourad Arous[c], Hajer Guermazi[a], Serge Agnel[d], Alain Toureille[d]

[a] Faculté des Sciences de Sfax, Département de Physique, BP 1171 Route de Soukra, 3018 Sfax, Tunisia
[b] Unité de Physique des Matériaux Isolants et Semi-isolants, Institut Préparatoire aux Etudes d'Ingénieur de Sfax, Route Menzel Chaker, km 0.5, BP 1172, 3018 Sfax, Tunisia
[c] Laboratoire des Matériaux Composites, Céramiques et Polymères, Faculté des Sciences de Sfax, Département de Physique, BP 1171 Route de Soukra, 3018 Sfax, Tunisia
[d] Groupe Energie et Matériaux (G E M), Université Montpellier 2, Place Eugène Bataillon, CC 079, 34095 Montpellier CEDEX 5, France

ARTICLE INFO

Article history:
Received 13 July 2009
Received in revised form
19 September 2009
Accepted 22 September 2009
Available online 25 September 2009

Keywords:
Polymer
Dielectric response
Ionic conduction

ABSTRACT

Thermally stimulated depolarization current (TSDC) and dielectric relaxation spectroscopy (DRS) techniques were employed to study the relaxations and the conductivity phenomena in epoxy-based polymer. In addition to the primary α relaxation process associated with the glass–rubber transition, significant interfacial relaxation and ionic conduction process have been revealed. The ac conductivity is temperature and frequency dependent and shows a dc plateau at low frequencies. Above the glass transition temperature, dc conductivity is described by a Vogel–Tamman–Fulcher–Hesse (VFTH) equation while it shows Arrhenius behaviour at higher temperatures.

Contents

1. Introduction

Epoxy resins form an important class of polymeric materials because of their good thermal and electrical properties. They have been used in a wide range of electric power installations and equipments. They are also employed as coatings and adhesives in civil engineering applications because of their good mechanical properties and strength of interaction with various substrates such as metals and glasses [1].

The most epoxy polymeric systems were prepared through the mixing in a stoichiometric weight ratio of epoxy resin and hardener. Usually they are considered as heterogeneous systems and their properties are strongly influenced by the ionic conductivity which dominates at low frequencies and high temperatures. There is increasing interest in the physical and technological properties of these polymers and a fine study of the dielectric relaxations and conductive behaviour is pertinent.

* Corresponding author at: Unité de Physique des Matériaux Isolants et Semi-isolants, Institut Préparatoire aux Etudes d'Ingénieur de Sfax, Route Menzel Chaker, km 0.5, BP 1172, 3018 Sfax, Tunisia. Tel.: +216 98 65 62 48; fax: +216 74 24 63 47.
E-mail address: hichem.smaoui@fss.rnu.tn (H. Smaoui).

0925-8388/$ – see front matter © 2009 Elsevier B.V. All rights reserved.
doi:10.1016/j.jallcom.2009.09.116

Dielectric relaxation spectroscopy (DRS) and thermally stimulated depolarization currents (TSDC) are two complementary techniques which are often used to reach a most complete knowledge of the relaxation and conduction mechanisms. By coupling these two techniques many works have been carried out to study dielectric relaxations in different materials [2–7].

DRS measures with high sensitivity the small changes in the dielectric properties of a material as a response to the application of a time dependent electric field. TSDC technique, which like DRS, has electrical character and is based on measuring the current occurring under thermal activation. More details of these techniques will be given respectively in Sections 2.2 and 2.3.

Previous studies [8–12] have been carried out in our laboratory to study the structural, electrical and optical properties of an epoxy-amine polymer. It has been demonstrated by means of TSDC, thermal step (TS) and IR spectroscopy techniques that this polymer presents a high polar character and the polarization depends strongly on its thermal history.

In the present work, TSDC and DRS techniques were employed to study over wide ranges of frequency and temperature the dielectric relaxations and the conductivity in this polymer.

2. Experimental

2.1. Sample preparation

The investigated epoxy polymer was prepared by mixing an epoxy resin and a hardener. The epoxy resin was a 2,2-bis (4-glycidyloxyphenyl) propane (molar mass 340 g/mol) and the hardener was a difunctional amine, supplied by Maestria. These two components were carefully and homogeneously mixed without any solvent in stoichiometry ratio to form a crosslinked structure. The mixture was stirred at room temperature, and then poured in parallelepipedal mould. The hardening was carried out at room temperature and under atmospheric pressure for 5 days.

2.2. TSDC technique

TSDC technique is based on a sample's depolarization by thermal activation [13,14]. Before TSDC measurements, samples were subjected to an electric poling. At a given temperature T_p (called poling or polarization temperature), a static electric field is applied to the investigated sample for a time t_p that is long enough to permit the different mobile entities in the material to orient themselves within the field. This configuration is then frozen by a rapid decrease in temperature keeping the electric field applied in order to avoid any relaxation of dipoles and/or charges. The field is then switched off and the sample is short circuited for a certain time to eliminate the eventual surface charges and stabilize sample at this temperature. The poled sample is then short-circuited through a high sensitive electrometer in an oven, which is programmed to rise linearly with time. During the linear increase of temperature, the return to equilibrium of the previously oriented entities generates a depolarization current which is recorded as a function of temperature. TSDC provides information on relaxation processes that occur in polymers. In contrast to the experimental simplicity of the TSDC technique, the experimental data analysis is not easy, as the polarization may be due to several microscopic processes (associated with dipolar or trapped charge mechanisms), whose relaxation will contribute to the depolarization current [15]. The current due to a dipole reorientation is given by the following expression [16]:

$$J(T) = A\ \exp\left[-\frac{E_a}{k_B T} - \frac{1}{\nu\tau_0}\int_{T_0}^{T} \exp\left(-\frac{E_a}{k_B T'}\right) \mathrm{d}T'\right] \quad (1)$$

where the pre-exponential factor A is given by: $A = Nm/\tau_0$ = constant and the relaxation time τ at temperature T is given by $\tau = \tau_0 \exp(E_a/k_B T)$ and E_a is the activation energy, k_B is the Boltzmann constant, T_0 is the initial temperature and T is the temperature at time t, ν is the rate of heating, τ_0 is the relaxation time at T_0, $m = q\delta$ is the dipole moment and N is the volume density of dipoles.

In the present work, samples were poled under an electric field (E_p) of 3 kV/mm during t_p = 3 h at poling temperatures T_p = 30 and 40 °C.

To perform TSDC measurements (80 mm × 80 mm × 1 mm) samples were coated on both sides with 4 cm diameter aluminum electrodes, deposited under vacuum. The depolarization currents were measured at a constant heating rate of 1 °C/min.

2.3. Dielectric relaxation spectroscopy (DRS)

Dielectric determination of the real permittivity ε' and the dielectric loss ε'' was performed on a dielectric thermal analyzer DEA 2970 from TA instrument over the temperature range from the ambient to 160 °C and a frequency interval from 10^{-1} to 10^6 Hz. The sample, with dimensions of about (10 mm × 10 mm × 0.5 mm), is placed between two gold parallel plate electrodes. The lower electrode, positioned on the surface of the furnace, applies the voltage that sets up the electrical field in the sample. A platinum resistance temperature detector (RTD) surrounds the perimeter of the gold electrode and measures the temperature of the sample. The upper electrode measures the generated current, which is then converted to an output voltage and amplified. A guard ring around the perimeter of the upper electrode corrects the electric field fringing and the stray capacitance at the edge of the plates. Dielectric measurements were performed using isothermal mode which consists on scanning frequencies at fixed temperature.

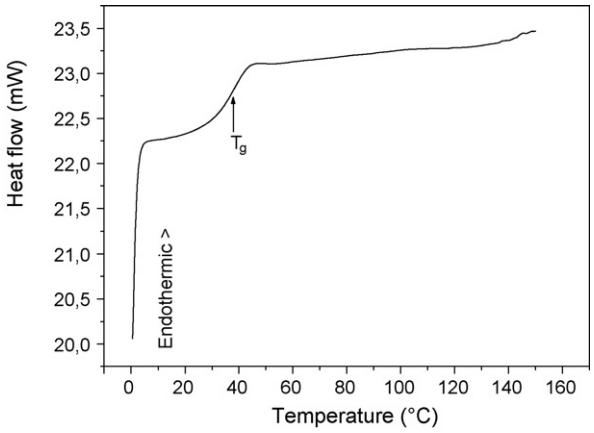

Fig. 1. DSC diagram obtained in the temperature range 0–150 °C at a heating rate of 10 °C min^{-1}.

3. Results and discussion

3.1. Differential scanning calorimetry

Differential scanning calorimetry measurements were performed with a Mettler DSC30 instrument, in the temperature range 0–150 °C. Fig. 1 shows the DSC diagram obtained at a heating rate of 10 °C/min after cooling from 150 to 0 °C at a cooling rate of 10 °C/min. The glass transition temperature of the investigated epoxy polymer appears around 37 °C.

3.2. Thermally stimulated depolarization current (TSDC)

TSDC measurements were performed, over the temperature range from 20 to 120 °C, on un-poled sample and samples poled at T_p = 30 and 40 °C. The current released from the un-poled sample during TSDC measurement is presented in Fig. 2(a). A weak spontaneous current peak appears around 35 °C (inset), which originate from dipolar disorientation associated with the glass–rubber transition as observed by DSC measurements.

The TSDC spectra of samples poled at T_p = 30 and 40 °C (Fig. 2(b) and (c)) show two overlapped relaxation peaks. The lower temperature peak around 48 °C corresponds to the α relaxation and the second one is attributed to the interfacial Maxwell Wagner Sillars relaxation (MWS) as examined in our previous paper [17]. It is due to the accumulation of charges at the interfaces during the polarization stage. Indeed, in previous work [11] we have demonstrated by means of Grazing incidence X-ray reflectometry measurements that the epoxy resin network presents locally a periodic arrangements with various spacing layers (from 32 to 74 nm). This creates interfaces in the epoxy network, which favors charge accumulation under applied field.

We noted that the α relaxation temperature was shifted to higher temperature (from 35 to 48 °C) in poled samples. In fact, samples have been poled at temperatures near T_g. At these temperatures, polymeric chains are more mobile, and then dipoles were easily oriented with the applied electric field during the polarization stage. The field was switched off after cooling samples to

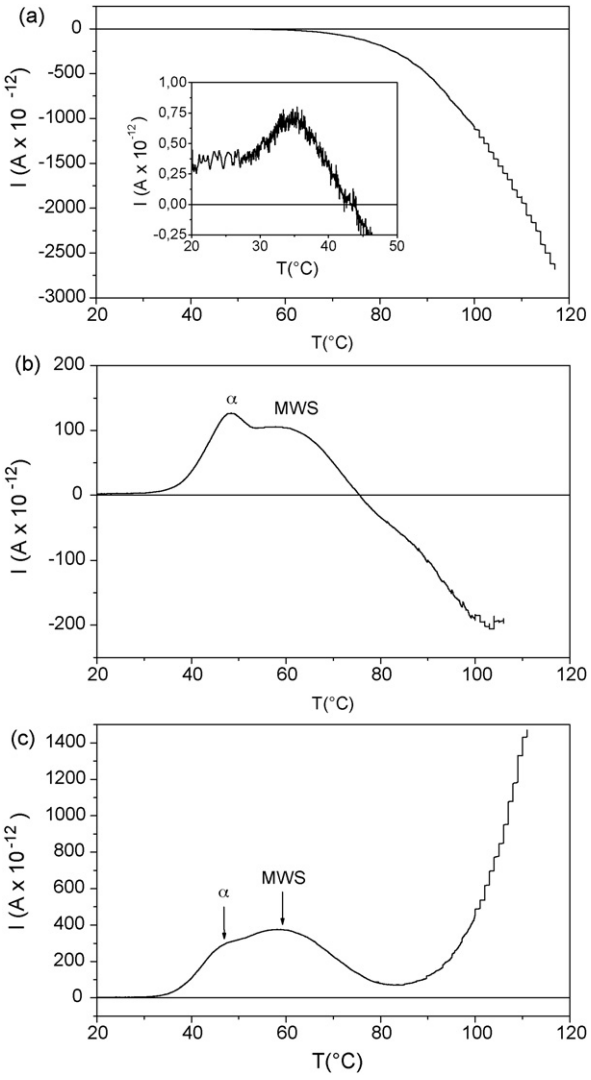

Fig. 2. TSDC spectra recorded on (a) the un-poled sample and after polarization process (E_p = 3 kV/mm during t_p = 3 h) at pooling temperatures (b) T_p = 30 °C and (c) T_p = 40 °C.

lower temperatures and consequently dipoles can be frozen in oriented state and then need more energy to relax during TSDC measurements, which explains the shift of α relaxation to higher temperature. To confirm this result, activation energies for the α dipolar relaxation have been determined from TSDC results by means of the initial slope method proposed by Bucci et al. [15]. In fact the expression for the thermally stimulated depolarization current at the beginning of the rise of the curve can be written as:

$$J(T) = A \exp\left(-\frac{E_a}{k_B T}\right) \quad (2)$$

A plot of $-Ln(J)$ versus $1/T$ is a straight line with a slope of E_a/k_B from which we can deduce the corresponding activation energy. Fig. 3 shows variations of $-Ln(J)$ versus $1000/T$ for the poled samples. The activation energies extracted from the slopes of the curves for the α dipolar relaxation are 227.18 kJ mol^{-1} (2.35 eV) for T_p = 30 °C and 276.67 kJ mol^{-1} (2.87 eV) for T_p = 40 °C. It can be notice that the activation energy increases with poling temperature.

Above the MWS relaxation peak temperature, TSDC currents of sample poled at T_p = 40 °C increase continuously with increasing temperature and reach high values at high temperatures, which is mainly due to the contribution of ionic conduction (this has

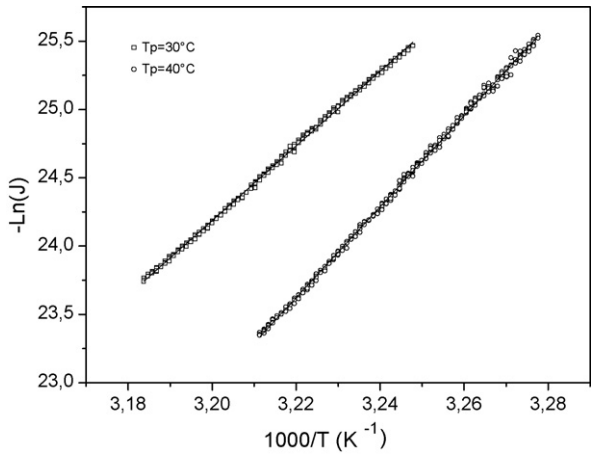

Fig. 3. Variation of $-Ln(J)$ versus $1/T$ for the α dipolar relaxation in samples poled at T_p = 30 and T_p = 40 °C.

been confirmed by reproducible TSDC measurements). Contrary, the TSDC spectra of the un-poled sample and sample poled at 30 °C (Fig. 2(a) and (b)) show a reversal of the currents sign above the relaxation peaks when temperature increases. Then currents increase rapidly with increasing temperature and reach high negative values. It appears that the sign of the current at the end of the TSDC spectrum depends on the poling temperature. Indeed, in the polarization process two mechanisms are operative, which are the orientation of polar groups with the applied electric field, and the space charge polarization. The disorientation of polar groups during the TSDC measurements gives rise to a current peak (α) which appears at temperature lower than the space charge polarization peak (MWS). At higher temperatures the space charge motion is accompanied with a creation of charge carriers which is due to ionization of impurities as well as the breaking of chemical bonds (epoxy ring-opening reaction, breaking of N–H bonds, etc.). In fact, in previous works [9,10] we have studied the effect of heating temperature on the space charge and structure of the epoxy polymer. We have found that the space charge density increases inside the material with increasing temperature. This was related to charge carriers creation due to structural changes. Thus, the thermally created charge carriers during TSDC measurements become more mobile at higher temperatures and constitute a homocurrent, which is opposite to the classical TSDC due to dipolar disorientation (heterocurrent). As the temperature is raised above the heteropeaks (α and MWS), the homocurrent starts increasing, as the number of thermally generated carriers increases and when this current is more important a reversal is observed from heterocurrent to homocurrent as shown in Fig. 2(b). If the poling temperature is higher, the charge carriers thermally generated during the polarization process are submitted to the effect of the poling electric field and thus give rise to a positive TSDC current as shown in Fig. 2(c).

3.3. Dielectric spectroscopy (DRS)

Real permittivity ε' and dielectric loss ε'' of the epoxy under investigation have been determined as a function of frequency (10^{-1} to 10^{6} Hz) in the temperature range from 30 to 160 °C. The curves depicting at various frequencies the dependence of the real permittivity ε' and the dielectric loss ε'' on temperature for the investigated polymer are shown in Fig. 4(a) and (b), respectively. For clarity reasons, the curves at other frequencies are not represented on these figures. A first inspection of the data reveals the presence of a main dipolar relaxation peak (Fig. 4(b)) which shifts slightly to higher temperatures when frequency increases. In Fig. 4(a), curves of $\varepsilon'(T)$ show that the α process is followed in

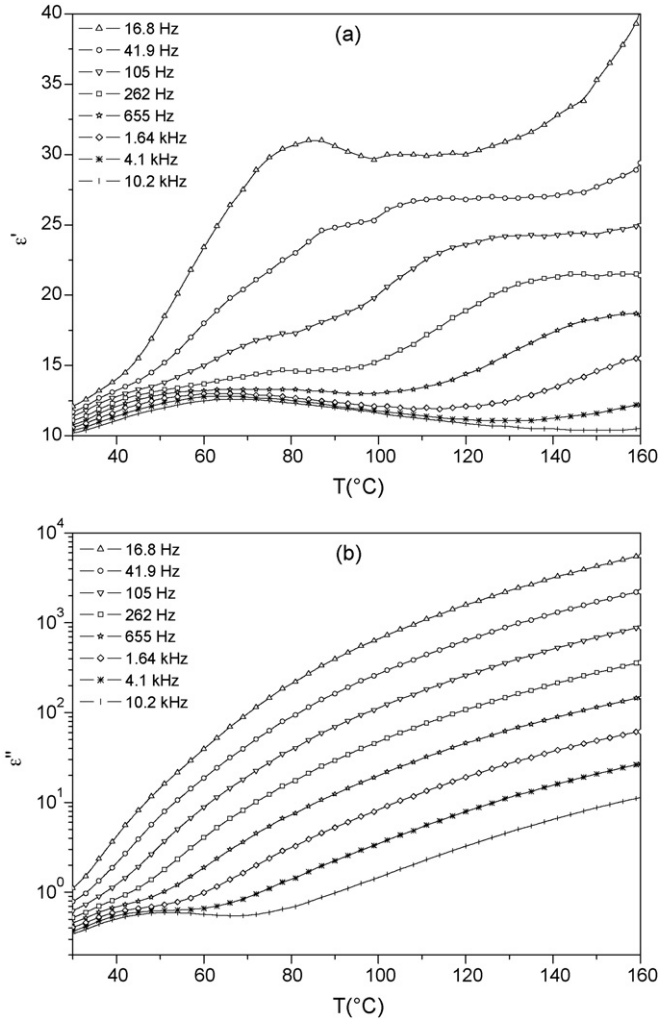

Fig. 4. Real permittivity ε' (a) and dielectric loss ε'' (b) versus temperature at various frequencies.

increasing temperature by two secondary phenomena which are caused by interfacial and ionic conduction processes. These two processes become dominant at low frequencies. At high frequencies the α relaxation peak is well defined in the isochronal representation of ε'' (Fig. 4(b)) and thus a plot of the frequency versus $1/T$ can be constructed. Fig. 5 shows a linear behaviour which can be fitted by the Arrhenius equation:

$$f = f_0 \exp\left(\frac{-E_a}{k_B T}\right) \quad (3)$$

where f_0 is a constant, k_B the Boltzmann constant and E_a is the activation energy of the relaxation process.

The activation energy value extracted from the fit is found to be 244 kJ mol^{-1} (2.53 eV). This relatively high value suggests that the α process is associated with the large scale motion at the glass transition.

Fig. 6(a) and (b) shows 3D plots of the real permittivity ε' and the dielectric loss ε'' versus frequency and temperature. Both real permittivity and dielectric loss are frequency and temperature dependent. When frequency decreases dielectric permittivity and dielectric loss become strongly dependent with temperature and reach high values at high temperatures, due to the dc conductivity effects. Indeed, at low frequencies and above T_g the double logarithmic plot of the dielectric loss versus frequency is a straight line with slope −1, indicating that the process is governed by conduc-

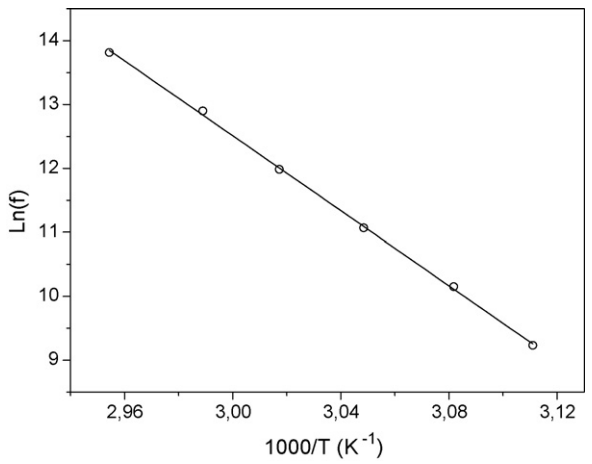

Fig. 5. Arrhenius plot of the frequency versus $1/T$ and the corresponding linear fit of the α relaxation process.

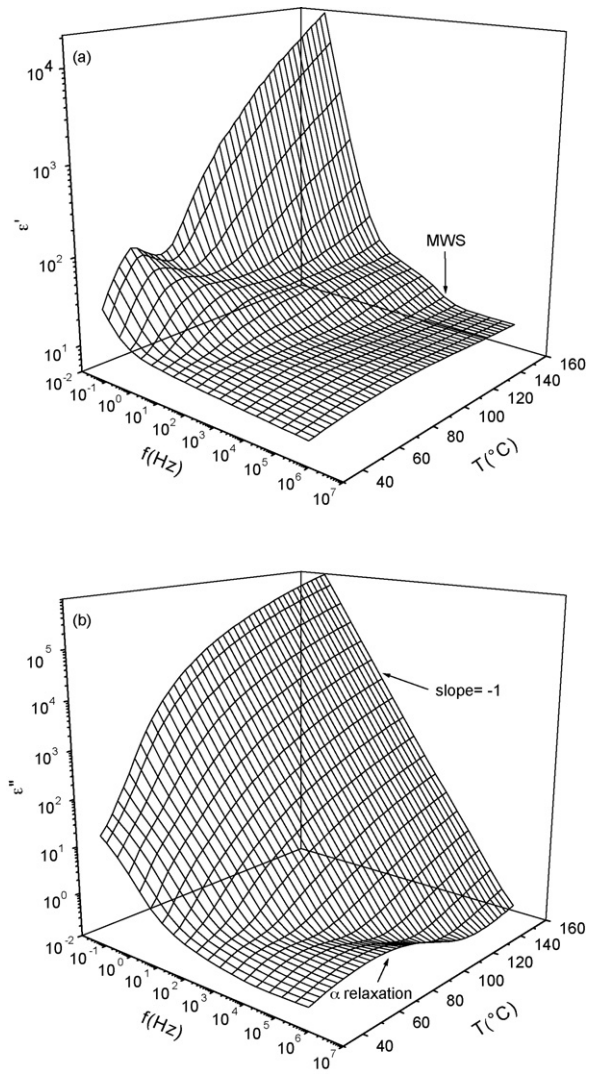

Fig. 6. Three-dimensional plots of the real permittivity (a) and dielectric loss (b) versus frequency and temperature.

tion [18–21]. This will be confirmed later by the corresponding ac conductivity plot. It can be noticed that even at relatively high frequencies, conductive effects still dominant at high temperatures (Fig. 6(b)). The inflection observed at high temperatures in the $\varepsilon'(f)$ representation (Fig. 6(a)) characterizing the interfacial relaxation process (MWS), shifts to lower frequencies as the temperature decreases. Due to the large conductive effects detected at high temperatures, curves of ε'' versus frequency do not show a loss peak associated with the MWS relaxation.

Owing to the large conductive effects it is preferable to express the dielectric results in terms of the complex electric modulus $M^* = 1/\varepsilon^*$. The values of the components of the complex permittivity were converted to the components of M^* by the following relations:

$$M* = M' + jM'', \quad j = (-1)^{1/2},$$

$$M' = \frac{\varepsilon'}{\varepsilon'^2 + \varepsilon''^2} \text{ and } M'' = \frac{\varepsilon''}{\varepsilon'^2 + \varepsilon''^2}. \tag{4}$$

Fig. 7 gives the temperature dependence of M'' at various frequencies. This figure confirms the presence of the three relaxations (α, MWS and conduction). Indeed α relaxation appears at high frequencies, while at low frequencies and in the low temperature region, conduction process appears as a shoulder which overlaps with the interfacial relaxation peak and the two processes merged into a large relaxation peak as the temperature increases. For temperatures above 120 °C, the relaxation process is due principally to interfacial and ionic conduction phenomena. To confirm these results, data of Fig. 8, giving the complex plane representation of M'' versus M' at various temperatures (36, 96, 120 and 150 °C), were fitted using the Havriliak–Negami equation given by the following [22]:

$$\varepsilon*(\omega) = \varepsilon_\infty + \frac{\varepsilon_s - \varepsilon_\infty}{(1 + (j\omega\tau)^\beta)^\gamma}, \quad 0 < \beta \text{ and } \gamma \le 1 \tag{5}$$

where ε_s and ε_∞ are the dielectric constants for the low and high frequency sides of the relaxation, β and γ are parameters describing the symmetric and asymmetric broadening of the relaxation time

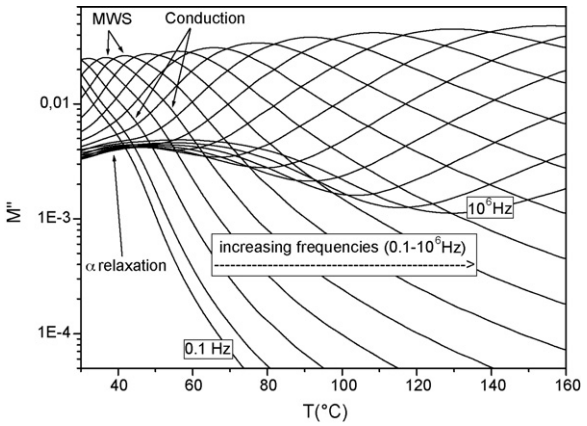

Fig. 7. Imaginary part of the electric modulus M'' versus temperature at various frequencies (10^{-1} to 10^6 Hz).

distribution, τ is the central relaxation time and ω is the angular frequency.

In the electric modulus formalism the Havriliak–Negami equations have the following form [23]:

$$M' = M_\infty M_s \frac{M_s D_1^2 + D_1 D_2 \cos\gamma\varphi}{M_s^2 D_1^2 + D_2[D_2 + 2M_s D_1 \cos\gamma\varphi]} \tag{6}$$

$$M'' = M_\infty M_s \frac{D_1 D_2 \sin\gamma\varphi}{M_s^2 D_1^2 + D_2[D_2 + 2M_s D_1 \cos\gamma\varphi]} \tag{7}$$

where $M_s = 1/\varepsilon_s$, $M_\infty = 1/\varepsilon_\infty$,

$$D_1 = \left[1 + (\omega\tau)^{2\beta} + 2(\omega\tau)^\beta \sin\frac{\beta\pi}{2}\right]^\gamma,$$

$$D_2 = (M_\infty - M_s)\left[1 + (\omega\tau)^\beta \sin\frac{\beta\pi}{2}\right]^\gamma$$

and

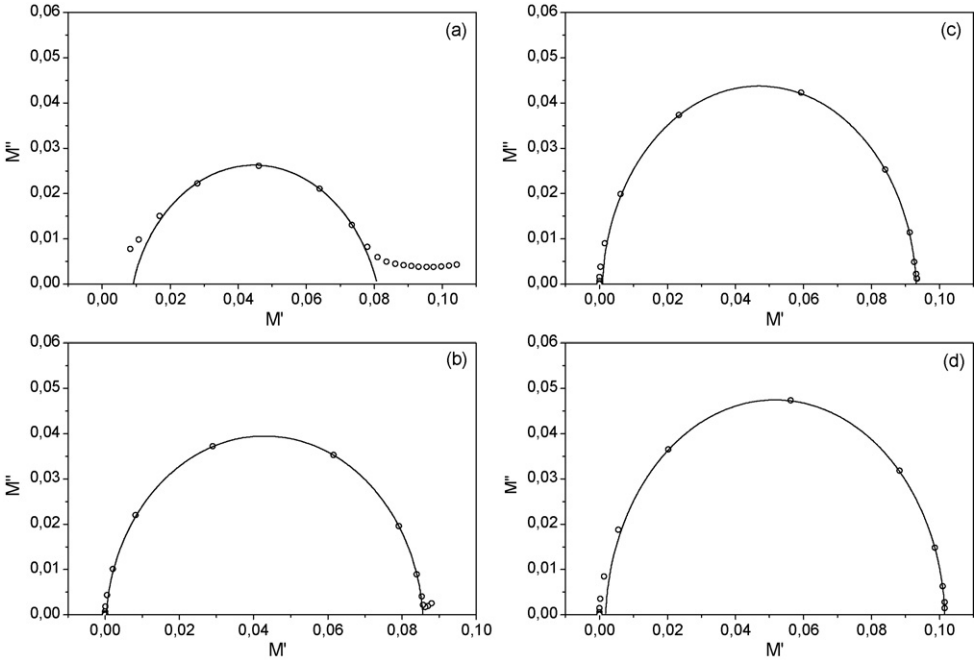

Fig. 8. Argand plots of the electric modulus at various temperatures: (a) 30 °C, (b) 96 °C, (c) 120 °C and (d) 150 °C. The solid lines are produced by the best fitting of the experimental data to the Haviliak–Negami approach for MWS relaxation.

Table 1
Parameters evaluated by fitting data according to the Havriliak–Negami approach for the MWS process.

T (°C)	β	γ	M_s	M_∞
36	0.828	0.963	0.0091	0.0809
96	0.97	0.981	0.00031	0.08563
120	0.985	0.984	0.00093	0.09312
150	0.976	0.996	0.001868	0.10157

$$(\omega\tau)^{\beta} = \frac{\tan[(1/\gamma)\arctan[(M_\infty M'')/(M_\infty M' - M''^2 - M'^2)]]}{\cos(\beta\pi/2) - \sin(\beta\pi/2)\tan[(1/\gamma)\arctan[(M_\infty M'')/(M_\infty M' - M''^2 - M'^2)]]}$$

All parameters evaluated by the fit are listed in Table 1. The theoretical semi-circles obtained by the fit and represented with solid lines in Fig. 8 correspond to the MWS process. When temperature increases experimental points move to the lower frequencies and reach the origin of the diagram contrary to the theoretical curves. This behaviour is due to the large effects of conduction. It can be noticed that for temperatures above 120 °C, experimental points coincide with the theoretical curves at the high frequency end. This demonstrates that at high frequencies and temperatures conduction and MWS relaxations are dominant. These results confirm those revealed from Fig. 7. The exponent γ informs on the asymmetry of the distribution of relaxation times, and the value $\gamma = 1$ corresponds to a symmetric distribution. The obtained values of this parameter (Table 1) are close to unity, assuming a symmetric shape of the relaxation times distribution. As temperature increases, exponent β approaches the unity indicating a near Debye type of the interfacial relaxation at high temperatures.

The ac conductivity has been calculated from the dielectric loss according to the following relation:

$$\sigma*(\omega) = j\varepsilon_0\omega\varepsilon*(\omega) = j\varepsilon_0\omega(\varepsilon' - j\varepsilon'') = \varepsilon_0\omega\varepsilon'' + j\varepsilon_0\omega\varepsilon' \quad (8)$$

The real part of $\sigma^*(\omega)$ is given by

$$\sigma_{ac}(\omega) = \varepsilon_0\omega\varepsilon'' \quad (9)$$

where $\varepsilon_0 = 8.85 \times 10^{-12}$ F m^{-1} is the permittivity of the free space and $\omega = 2\pi f$ the angular frequency.

Fig. 9 depicts at various temperatures the dependence of the ac conductivity on frequency. The ac conductivity is clearly temperature and frequency dependent and increases with increasing frequency and temperature. Its variation shows a flat plateau at low frequencies and high temperatures. As temperature decreases, the dc plateau decreases and σ_{ac} becomes strongly dependent on frequency at the high frequency end.

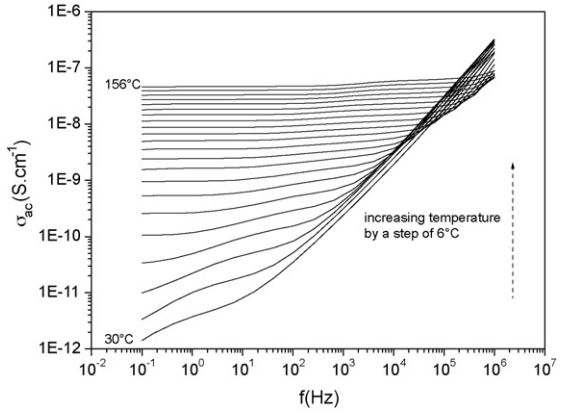

Fig. 9. Real part of ac conductivity versus frequency at various temperatures.

Table 2
Parameters corresponding to Vogel–Fulcher–Tamman–Hesse (VTFH) equation of the dc conductivity in the temperature range from 51 to 108° C.

VTFH parameters	
A (S/cm)	7.69×10^{-7}
B (K)	487.04
T_0 (K)	272.15

Values of dc conductivity (σ_{dc}), determined at several temperatures above the glass transition temperature, were used to construct plot of Fig. 10(a). The obtained results show, a linear behaviour at high temperatures (from 117 to 160 °C) and a non-linear one elsewhere (from 51 to 108 °C). Indeed, at high temperatures (117–160 °C), data of Fig. 10(b) are well fitted by an Arrhenius equation similar to Eq. (3). While data in the temperature range from 51 to 108 °C (Fig. 10(c)) are best fitted with the Vogel–Tammann–Fulcher–Hesse (VTFH) equation [24–26]:

$$\sigma_{dc} = A\ \exp\left(-\frac{B}{T - T_0}\right) \quad (10)$$

where empirical parameters A, B and T_0 are temperature independent.

This result indicates that in the temperature range from 51 to 108 °C, conduction mechanism is governed by the motion of polymeric chains, as it has often been observed in polymers above T_g temperature [27–29]. While at higher temperatures ionic conduction is dominant as observed on TSDC spectra, and it was described by Arrhenius law.

The VTFH parameters deduced from the best fit are summarized in Table 2. The Vogel temperature T_0 has been found in many polymers to be in the range of about 50 K below T_g [2,6,29,30], which is approximately the case of the epoxy resin studied here.

At high temperatures the activation energy determined from the Arrhenius equation for the dc conductivity is about 45.41 kJ mol^{-1} (Table 3). The activation energy of the dc conductivity at low temperature (from 51 to 108 °C) does not appear directly in the VTFH equation but has to be calculated from the following relation [2,30,31]:

$$E_a = RB\left(\frac{T}{T - T_0}\right)^2 \quad (11)$$

where R is the gas constant. The obtained values at different temperatures are summarized in Table 3. We noted that the activation energy of ionic conduction mechanism is lower than ones characterizing the conduction due to polymeric chain motion. It can be concluded that in the whole temperature range, activation energies of the dc conductivity are lower than the α process ones. This might be due to the low crosslinking density of the epoxy system. Indeed, the studied polymer has a low T_g value (37 °C), and it has been reported that the high crosslinking density is directly related to the high value of the glass transition temperature T_g [32–34].

Table 3
Activation energies of the dc conductivity (σ_{dc}).

	T (°C)	E_a (kJ mol^{-1})
VTFH model	51	158.13
	60	121.28
	75	85.24
	90	64.65
	105	51.64
Arrhenius law	117–160	45.41

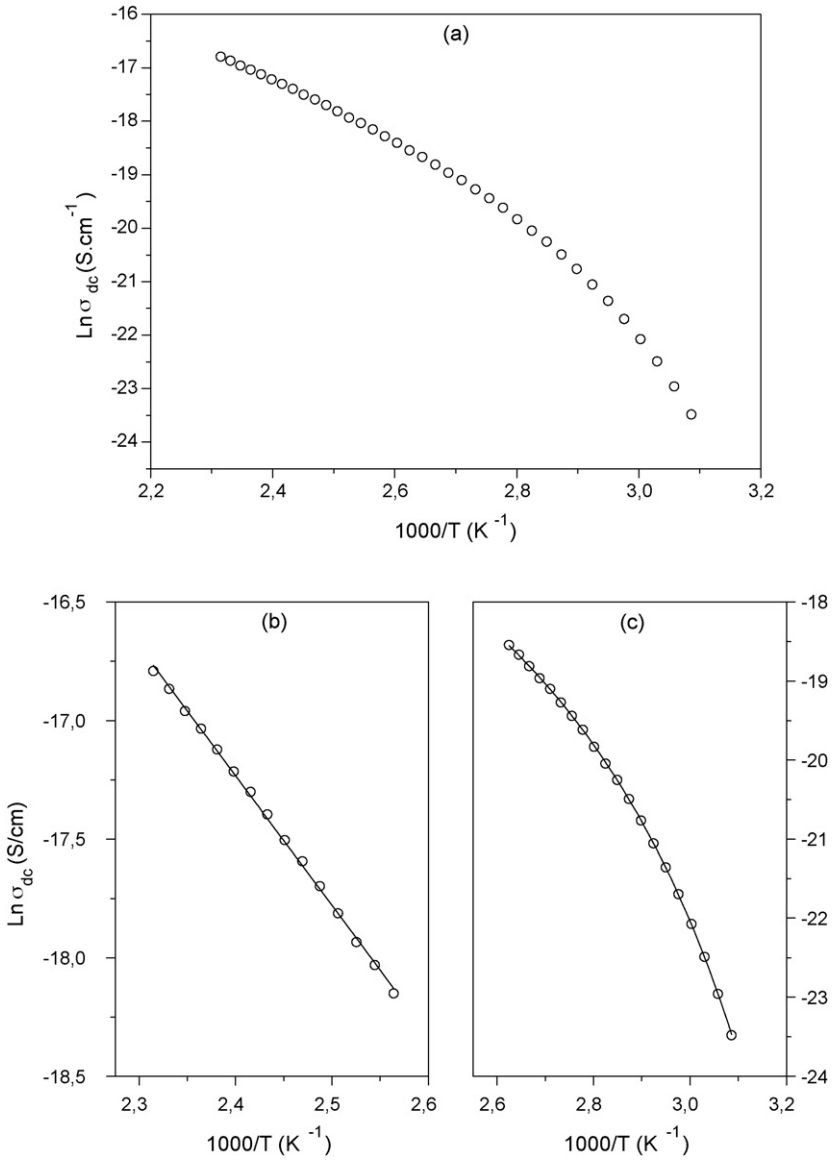

Fig. 10. (a) Dependence of dc conductivity on the temperature for the epoxy polymer. The lines are best fit of the: Arrhenius equation to the data of (b) and VTFH equation to the data of (c).

4. Conclusion

In this paper dielectric relaxations and conductivity have been studied by means of thermally stimulated depolarization current (TSDC) and dielectric relaxation spectroscopy (DRS) measurements. TSDC depolarization processes were found to be dependent on the experimental conditions.

In addition to the α dipolar relaxation, interfacial or Maxwell Wagner Sillars (MWS) relaxation is evident in the TSDC and dielectric spectra of the studied epoxy polymer. The distribution of relaxation times associated with the interfacial relaxation is found to be symmetric and approaches the Debye type at high temperatures.

A spontaneous homocurrent originating from the movement of the thermally generated charge carriers is observed on the TSDC spectra. This current has an opposite sign than the heterocurrent due to dipolar disorientation. The sign of the resultant current above the relaxation of hetero-peaks depends on the pooling temperature. TSDC reveals the contribution of ionic conduction at high temperatures. DRS results have shown that ionic conduction is significant at low frequencies and high temperatures.

It was observed that, above the glass transition temperature, the dc conductivity follows a Vogel–Tammann–Fulcher–Hesse (VTFH) behaviour while it shows an Arrhenius behaviour at high temperatures. The low value of the activation energy of the dc conductivity was related to a low crosslinking density of the polymer.

Acknowledgments

The authors acknowledge the financial support of the 'Ministère de l'Enseignement Supérieur, de la Recherche Scientifique et de la Technologie', Tunisia and ICTP through TWAS Grant no. 00-043 RG/PHYS/AF/AC.

References

[1] G. Rabilloud, High-Performance Polymers (1) Conductive Adhesives Chemistry and Applications, Editions Technip, Paris, 1997.
[2] J. Belana, J.C. Canadas, J.A. Diego, M. Mudarra, R. Diaz-Calleja, S. Friederichs, C. Jaimes, M.J. Sanchis, Polym. Int. 46 (1998) 11–19.
[3] G. Georgoussis, A. Kanapitsas, P. Pissis, Y.V. Savelyev, V.Y. Veselov, E.G. Privalko, Eur. Polym. J. 36 (2000) 1113–1126.

[4] P. Pissis, G. Georgoussis, V.A. Bershtein, E. Neagu, A.M. Fainleib, Dielectric studies in homogeneous and heterogeneous polyurethane/polycyanurate interpenetrating polymer networks, J. Non-Cryst. Solids 305 (2002) 150–158.
[5] S. Kripotou, P. Pissisa, V.A. Bershtein, P. Sysel, R. Hobzova, Polymer 44 (2003) 2781–2791.
[6] L. Delbreilh, E. Dargent, J. Grenet, J.M. Saiter, A. Bernès, C. Lacabanne, Eur. Polym. J. 43 (2007) 249–259.
[7] P. Saxena, M.S. Gaur, P. Shukla, P.K. Khare, J. Electrost. 66 (2008) 584–588.
[8] H. Smaoui, H. Guermazi, S. Agnel, Y. Mlik, A. Toureille, Polym. Int. 49 (2000) 1513–1518.
[9] H. Guermazi, H. Smaoui, S. Agnel, Y. Mlik, A. Toureille, F. Schué, Polym. Int. 50 (2001) 743–747.
[10] H. Smaoui, H. Guermazi, S. Agnel, Y. Mlik, A. Toureille, F. Schué, Polym. Int. 52 (2003) 1287–1293.
[11] H. Medhioub, C. Zerrouki, N. Fourati, H. Smaoui, H. Guermazi, J.J. Bonnet, J. Appl. Phys. 101 (2007) 043509.
[12] H. Medhioub, H. Smaoui, N. Fourati, C. Zerrouki, H. Guermazi, J.J. Bonnet, J. Phys. Chem. Solids 69 (2008) 2476–2480.
[13] J. Van Turnhout, Thermally Stimulated Discharge of Polymer Electrets, Elseiver, Amesterdam, 1975.
[14] V.M. Gun'ko, V.I. Zarko, E.V. Goncharuk, L.S. Andriyko, V.V. Turov, Y.M. Nychiporuk, R. Leboda, J. Skubiszewska-Zieba, A.L. Gabchak, V.D. Osovskii, Y.G. Ptushinkii, G.R. Yurchenko, O.A. Mishchuk, P.P. Gorbik, P. Pissis, J.P. Blitz, Adv. Colloid. Inter. Sci. 131 (2007) 1–89.
[15] C. Bucci, R. Fieschi, C. Guidi, Phys. Rev. 148 (2) (1966) 816–823.
[16] J. Vanderschueren, J. Gasiot, in: P. Braunlich (Ed.), Thermally Stimulated Relaxation in Solids, Springer-Verlag, Berlin, 1979.
[17] H. Smaoui, L.E.L. Mir, H. Guermazi, S. Agnel, A. Toureille, J. Alloys Compd. 477 (2009) 316–321.
[18] R. Diaz-Calleja, E. Riande, J. San Roman, V. Compan, Macromolecules 27 (1994) 2092–2101.
[19] A. Garcia-Bernabe, R. Diaz-Calleja, A. Bello, E. Perez, Polymer 42 (2001) 6793–6800.
[20] Y. Sun, Z. Zhang, C.P. Wong, Polymer 46 (2005) 2297–2305.
[21] P.S. Anantha, K. Hariharan, Mater. Sci. Eng. B 121 (2005) 12–19.
[22] S. Havriliak, S. Negami, Polymer 8 (1967) 161–210.
[23] M. Arous, I.Ben. Amor, A. Kallel, Z. Fakhfakh, G. Perrier, J. Phys. Chem. Solids 68 (2007) 1405–1414.
[24] H. Vogel, Phys. Z 22 (1921) 645.
[25] G.S. Fulcher, J. Am. Ceram. Soc. 8 (1925) 339–355.
[26] G. Tammann, W. Hesse, Z. Anorg. Allg. Chem. 156 (1926) 245.
[27] P. Pissis, A. Kanapitsas, Yu.V. Savelyev, E.R. Akhranovich, E.G. Privalko, V.P. Privalko, Polymer 39 (1998) 3431–3435.
[28] A. Kanapitsas, P. Pissis, R. Kotsilkova, J. Non-Cryst. Solids 305 (2002) 204–211.
[29] A. Kanapitsas, P. Pissis, C.G. Delides, P. Sysel, V. Sindelar, V.A. Bershtein, Polymer 43 (2002) 6955–6963.
[30] E. Bureau, C. Cabot, S. Marais, J.M. Saiter, Eur. Polym. J. 41 (2005) 1152–1158.
[31] M.J. Sanchis, R. Diaz-Calleja, C. Jaimes, J. Belana, J.C. Canadas, J.A. Diego, M. Mudarra, J. Sellarès, Polym. Int. 53 (2004) 1368–1377.
[32] T. Sasuga, A. Udagawa, Polymer 32 (3) (1991) 402–408.
[33] F. Henn, J.C. Giuntini, J.L. Halary, J. Vanderschueren, J.M. Muracciole, IEEE Trans. Dielect. Electr. Insul. 7 (4) (2000) 551–555.
[34] L. Nunez, S. Gomez-Barreiro, C.A. Gracia-Fernandez, M.R. Nunez, Polymer 45 (2004) 1167–1175.